RESEARCH MEMORANDUM

PRELIMINARY RESULTS FROM A FREE-FLIGHT INVESTIGATION OF BOUNDARY-LAYER TRANSITION AND HEAT TRANSFER ON A HIGHLY POLISHED 8-INCH-DIAMETER HEMISPHERE-CYLINDER AT MACH NUMBERS UP TO 3 AND REYNOLDS NUMBERS BASED ON A LENGTH OF 1 FOOT UP TO 17.7×10^6

By James R. Hall, Katherine C. Speegle, and Robert O. Piland

Langley Aeronautical Laboratory
Langley Field, Va.

NATIONAL ADVISORY COMMITTEE FOR AERONAUTICS

WASHINGTON

May 16, 1957

NATIONAL ADVISORY COMMITTEE FOR AERONAUTICS

RESEARCH MEMORANDUM

PRELIMINARY RESULTS FROM A FREE-FLIGHT INVESTIGATION OF BOUNDARY-LAYER TRANSITION AND HEAT TRANSFER ON A HIGHLY POLISHED 8-INCH-DIAMETER HEMISPHERE-CYLINDER AT MACH NUMBERS UP TO 3 AND REYNOLDS NUMBERS BASED ON A LENGTH OF 1 FOOT UP TO 17.7×10^6

By James R. Hall, Katherine C. Speegle,
and Robert O. Piland

SUMMARY

Measurements of bee-layer transit ion and aerodynamic heat transfer have been made on an 8-inch-diameter hemisphere -cylinder rocket - propelled free-f light model. Preliminary results are presented herein for the portion of the flight at high Reynolds numbers. Data in the form of Stanton numbers are presented for Mach numbers between 2 and 3 for free-stream Reynolds numbers based on a length of 1 foot between 10.7×10^6 and 17.7×10^6.

It was shown that surface roughness has a first-order effect on the Reynolds number of transition. Comparison with previous tests indicated that the Reynolds number of transition breed on momentum thickness on the hemisphere could be increased from the order of 100 to 400 to the order of 900 to 1,200 by reducing the roughness from greater thsn 25 rms micro-inches to less than 5 microfiches for these test conditions. It was further shown that local roughness was likely to be more important than average roughness.

INTRODUCTION

The National Advisory Committee for Aeronautics is conducting a series of flight tests to study the aerodynamic heating characteristics of blunt shapes. Initial flight tests of blunt shapes in the Mach number range of 2 to 5 indicated that boundary-layer transition occurs at

local Reynolds numbers based on distance from the stagnation point of 1×10^6 to 2×10^6. The Reynolds number of transition based on calculated momentum thickness was in the range of 100 to 400. It was conjectured that surface roughness was causing the very low transition Reynolds number, the surface roughness of the models being 25 rms microinches or greater. The results of these initial tests are presented in references 1 and 2.

In order to find the gross effect of roughness on transition, several highly polished blunt noses have been tested. The first of these, reported in reference 3, had a surface roughness of 2 to 5 microinches. The local Reynolds number of transition was as high as 15×10^6 and never lower than 4.5×10^6 for the period-of flight during which data were obtained. These Reynolds numbers correspond to Reynolds numbers based on momentum thickness of 2,100 and 800, respectively. In either case a large beneficial effect of polishing is indicated. The present report contains preliminary results from a second flight test of a highly polished nose. The model was an 8-inch-diameter hemisphere-cylinder identical to the "rough" hemisphere-cyltider reported in reference 2. Again the purpose of the test was to determine the gross effect of surface roughness on transition. The present preliminary report contains data obtained only dining the portion of flight at high Reynolds numbers based on a length of 1 foot (first-stage boost and coast) and only on the forward portion of the model. Data are presented for Mach numbers up to 3 and Reynolds numbers based on diameter up to 12×10^6. The test was conducted in December 1956 at the Langley Pilotless Aircraft Research Station at Wallops Island, Va.

SYMBOLS

h	aerodynamic heat-transfer coefficient, Btu/(sec)(sq ft)($^\circ$F)
c_p	specific heat, Btu/slug-$^\circ$F
k	thermal conductivity of air, Btu/(sec)(sq ft)($^\circ$F)/ft
μ	viscosity of air, slugs/ft-sec
ρ	density, slugs/cu ft
M	Mach number
v	velocity, ft/sec

N_{St} Stanton number, $\frac{h}{c_p \rho V}$

P pressure, lb/sq ft

N_{Pr} Prandtl number, $\frac{c_p \mu}{k}$

R Reynolds number, $\frac{\rho V l}{\mu}$

T *temperature*

D diameter of model, ft

l distance from stagnation point along surface of model, in.

x distance from stagnation point along axis of model, in.

b distance from stagnation point to hemisphere-cylinder junction, $\frac{\pi D}{4}$

e angle between stations on hemisphere and stagnation point, deg

t time, sec

T wall thickness, ft

Subscripts:

au adiabatic wall

so isentropic stagnation

v just outside boundary layer

l based on distance from stagnation point along surface of model

w pertaining to wall material

m undisturbed free stream ahead of model

1 based on length of 1 foot

MODEL, INSTRUMENTATION, AND FLIGHT TEST

The general model arrangement and pertinent dimensions of the test vehicle are shown in the sketch of figure 1 and in the photograph of figure 2. The body was an 8-inch-diameter hemisphere-cylinder having a fineness ratio of 17.25, stabilized by three tapered trapezoidal magnesium fins equally spaced and welded to the cylindrical body at the 91.4-percent body station. The leading edges of the fins were capped with 0.032-inch Inconel to protect the magnesium from excessive aerodynamic heating. Details of the fins are given in figure 1.

The model was all metal in construction. Spun Inconel was utilized for the *nose* section which comprised 20.5 percent of the body length. The rear section was formed from magnesium-alloy skin and a cast magnesium-alloy tail section to which the fins were welded. Skin thicknesses for each measuring station are shown in table I. The Inconel portion of the model was superpolished to a roughness of 1 to 5 microinches on the hemispherical dome as measured by an interference microscope. The degree of polish on the cylinder gradually degenerated to 3 *to* 8 microfiches at the rearmost portion of the Inconel skin. It was noted that imperfections of undetermined depth existed at the hemisphere-cylinder juncture. The degree of polish is indicated in figure 3. The model was boosted by an M5 JATO rocket motor and sustained by a 2.8-B-8100 Cajun rocket motor carried internally. A photograph of model and booster is shown in figure 4.

Instrumentation

The model was equipped with six channels of telemetering, two of which transmitted wall temperatures, and four transmitted accelerations to a ground receiving station. The four accelerometers were to measure longitudinal (two), normal, and transverse acceleration. The temperature channels were commutated approximately every 0.2 second to *transmit* temperature measurements at the locations shown in table I. Thermocouples 1 to 20 were installed in the Inconel nose section along two rays 180° apart by welding the chromel-alumel thermocouples to the inner surface. The accuracy of the temperature measurements was within ±2 percent of full scale. Full scale for this test was 1,400° F; therefore, an error of ±28° *was* possible. A more complete discussion of the general methods of the temperature-telemetering techniques employed is presented in reference 4. The stagnation-patit thermocouple measurements are not discussed herein, since this paper is devoted to transition at high Reynolds numbers.

In addition to the instrumentation carried internally, the model was tracked by a CW Doppler velocimeter snd an NACA modified SCR-584 *radar* to determine the trajectory. Atmospheric and wind conditions were determined by means of radiosondes launched near the time of flight and tracked by a Rawin set AN/GMD-1A.

Test

The model was launched at an elevation angle of 70°. The booster accelerated the model to a Mach number of 2.96. The model with burned-out booster still attached coasted upwards for a predetermined time until the sustainer rocket motor fired. Data in this report are confined to the first-stage boost (t = 0 to 3.5 seconds) and the coasting period between 4.0 and 6.0 seconds.

DATA REDUCTION

S--temperature measurements were telemetered to the ground receiving station. Model Mach number, velocity, and altitude (fig. 6(a)) were determined from SCR-584 position radar measurements and Doppler velocimeter measurements. Static conditions of temperature, density, and pressure (fig. 6(b)) were determined by correlating radiosonde and SCR-584 position-radar measurements.

This information was reduced to the form of Stanton number by using the following relationship:

$$N_{St,v} = (c_p \rho V)_v = \frac{1}{(c_p \rho V)_v} \left[\frac{\rho_w T_w c_{p,w} \frac{dT_w}{dt}}{(T_{aw} - T_w)} \right]$$

Radiation and conduction effects were estimated and found to be small snd are therefore neglected in this preliminary report. The skin thickness T_w was measured and is presented in table I. The density ρ_w of Inconel is constant. The specific heat $c_{p,w}$ varies with skin temperature as shown in reference 5. The rate of change of temperature with time dT_w/dt was read mechanically from the measured temperature data of figure 5. The thermodynamic properties of air used in the computations-were-obtained from reference 6. The adiabatic wall temperature T_{aw} was obtained from the definition of recovery factor

$$\text{Recovery factor} = \frac{T_{aw} - T_v}{T_{so} - T_v}$$

This leads to

$$T_{aw} = T_v + N_{Pr}^{1/3}(T_{so} - T_v)$$

The turbulent recovery factor is considered to be equal to $N_{Pr}^{1/3}$ and the laminar recovery factor is considered to be equal to $N_{Pr}^{1/2}$, both based on wall temperature. The stagnation temperature T_{s_o} was obtained with the assumption of perfect gas.

Local conditions were obtained by using pressure distributions for a hemisphere-cylinder presented in reference 7 and from supersonic flow relations for normal shocks (ref. 8).

RESULTS AND DISCUSSION

General

Local heat-transfer coefficients (Stanton numbers) were reduced from the temperature histories and associated data as described in the section entitled "Data Reduction." The Stanton numbers are presented in figure 7 as a function of l/b and θ. Each part of figure 7 presents data obtained at a given time during the flight corresponding to a certain Mach number and Reynolds number condition. The times and conditions for which data are presented are as follows :

	t, sec	M_∞	$R_{\infty,1}$
Power on (accelerating flight)	2.5	2.14	13.7X 10^6
	3.0	2.73	17.0
	3.5	2.96	17.7
Power off (coasting flight)	4.0	2.78	15.9 x 10^6
	5.0	2.42	12.7
	6.0	2.17	10.7

Figures 7(a) to 7(c) present data for the power-on accelerating flight, during which time Mach number and Reynolds number based on a length of 1 foot increase to 2.96 and 17.7 x 10^6, respectively. Figures 7(d) to 7(f) present data for the coasting decelerating portion of

the flight as the Mach number and Reynolds number based on a length of 1 foot decrease to 2.17 and 10.7×10^6, respectively.

The laminar theories of references 9 and 10 and the turbulent flat-plate theory of reference 11 are also presented in figure 7. Boundary-layer-transition location as indicated by an abrupt and large increase in Stanton number is pointed out on each figure and the transition Reynolds numbers are noted.

Transition

Description of transition movement.- At the earliest time (t = 2.5 seconds, fig. 7(a)) at which data were obtained, transition occurs at $\theta = 75^\circ$ ($l/b = 0.833$). Transition remains at this location until t = 3.5 seconds (fig. 7(c)), at which time it moves to $\theta = 60^\circ$ (Z/b = 0.667). During this time (t = 2.5 to 3.5 seconds) the local Reynolds number of transition based on calculated momentum thickness increased slightly from 1,100 to 1,200 and then decreased to 940. The local Reynolds number of transition based on distance from the stagnation point varied from 4.6×10^6 to 4.3×10^6 to 4.4×10^6. Stanton numbers reduced from both rays (0° and 180°) of thermocouples agreed in showing the location of transition during this period.

After t = 3.5 seconds the model decelerates and Mach number and Reynolds number decrease. Transition moves rearward and at t = 4.0 seconds (fig. 7(d)) Stanton numbers reduced from the 180° ray of thermocouple measurements indicate transition at $\theta = 90^\circ$ (Z/b = 1) while measurements from the 0° ray show transition far back on the cylinder at $l/b = 3.23$. This condition remains throughout t = 6 seconds (fig. 7(f)), the only change being that the transition point moves from $l/b = 3.23$ to $l/b = 2.6$. Normal and transverse accelerometers show that the model was flying at nearly zero ($\pm 0.4^\circ$) angle of attack during this period of the flight, thereby precluding the angle of attack as a possible explanation for the different locations of transition on opposite sides of the missile. Since the flow is laminar to Z/b = 2.6 to 3.23 on one side of the model, there is obviously no aerodynamic (Mach number, Reynolds number, heating, and so forth) parameter causing transition at $\theta = 90^\circ$ on the opposite side; therefore, a physical disturbance (local roughness) is considered to be the cause of transition at $\theta = 90^\circ$. The possible contamination effects of this local roughness are discussed in a subsequent section. The Reynolds number of transition between t = 4 and 6 seconds on the bottom side varied between 1,470 and 1,270 based on calculated momentum thickness and between 15.1×10^6 and 9.9×10^6 based on distance from the stagnation point.

Comparison with previous test results.- Reference 2 presents aerodynamic heating and transition data from a previous flight test of an

8-inch-diameter hemisphere-cylinder rocket model. The first portion of this previous flight test was very similar to the present model in the variation of Mach number and Reynolds number. The major difference between the two models was the surface roughness. Whereas the present model had a roughness of 1 to 5 microinches, the previous model had a surface roughness greater than 25 rms microinches. Transition on the "rough" model during power-on flight' (t = 0 to 3.75 seconds) occurred at local Reynolds numbers between 0.5 x 10^6 and 2 x 10^6 based on distance from the stagnation petit or between 150 and 300 based on calculated momentum thickness. These values compare with values of 4.4 x 10^6 end 900 to 1,200, respectively, for the present test (figs. 7(a) to 7(c)). The conclusion is obvious: reducing the surface roughness had a large effect on the transition Reynolds number when the Reynolds number based on a length of 1 foot was high enough to cause transition on this hemisphere.

Turbulence from the bottom side ($t \geq 4$ seconds, $\theta = 90^\circ$, Z/b . 1) did *not have a large effect on* transition on the opposite side. This is evidenced by the fact that location of transition after leaving a position on the nose was the same for the "smooth" and the "rough" models, that is, 2/b = 3.25. It was observed that local roughness at the $\theta = 90^\circ$ ($l/b = 1$) point of the "smooth" model was greater than the >25 rms microinch finish of the "rough" model. These imperfections could not be removed by polishing and were worse then similar local. bad spots on the rough model.

Reference 3 presents heating and transition measurements on a highly polished (2 to 5 microinches) hemisphere-cone model. This test resulted in local Reynolds numbers of transition as high as 1,900 to 2,100 based on momentum thickness or 15 x 10^6 based on distance from stagnation point. However, as the Reynolds number based on a length of 1 foot increased, transition moved forward and R_θ and $R_{v,l}$ dropped to 800 and 5x 10^6, respectively. This lower value of transition Reynolds number is of the same order as the minimum Reynolds number of transition measured in the present test. Some quantitative observations may be made from these two tests for blunt noses having surface finishes of 1 to 5 microinches. Laminar flow may be obtained at Reynolds numbers based on momentum thickness as high as 1,500 to 2,000 on the hemisphere, but with Reynolds numbers based on a length of 1 foot of the order of 18x10^6, values of 800 seem to be a more reasonable value at which to expect transition to occur.

It has been conjectured that the model surface becomes roughened in flight and results in a "jump" in transition location. Reference 3, which showed a "jump" from R_θ of 2,100 to R_θ of 800 in a very short period of time, tended to support this conjecture. The present test, however, would indicate the opposite. First, the movement of transition seems closely allied with Reynolds number based on a length of 1 foot, which indicates that no large local roughness suddenly appeared; and, second, when the model decelerated, transition Reynolds numbers were as

high as during accelerating flight, indicating the absence of a progressive increase in average surface roughness which would have moved transition gradually forward with time for given conditions.

Heat-transfer coefficients.- The heat-transfer coefficients of laminar magnitude appear to agree reasonably well with the laminar theories of references 9 and 10, especially beyond $\theta = 30°$. The turbulent data when faired are in fair agreement with flat-plate theory of reference 11. It is significant that the turbulent values at the transition point are not appreciably or consistently higher than theory.

CONCLUDING REMARKS

A highly polished 8-inch-diameter hemisphere-cylinder has been flight tested to obtain boundary-layer transition and aerodynamic heating information. Preliminary results of this flight test are presented herein for the portion of the flight at high Reynolds numbers based on a length of 1 foot. Data are presented in the form of Stanton numbers for Mach numbers between 2 and 3 for free-stream Reynolds numbers based on a length of 1 foot between 10.7×10^6 and 17.7×10^6. The following observations were made from the present data and comparisons with previous tests in this program:

1. Laminar flow on the hemisphere was obtained to local Reynolds numbers based on momentum thickness as high as 1,200. At the highest Reynolds number based on a length of 1 foot of 17.7×10^6 the local Reynolds number of transition was 940.

2. The effect of reducing the surface roughness from greater than 25 rms microinches to less than 5 microfiches was to increase transition Reynolds numbers from between 100 and 400 to values from 940 to 1,200.

3. This minimum Reynolds number of transition (940) is in good agreement with results presented in NACA Research Memorandum L57D05 for a blunt nose of about the same surface finish (2 to 5 microinches), indicating the repeatability of transition location in practical application.

4. It appeared that a local roughness condition caused transition on one side of the cylinder during a portion of the flight. The location of transition on the opposite side of the model was not apparently

affected to any large extent by contamination from turbulence emanating from this point.

Langley Aeronautical Laboratory,
National Advisory Committee for Aeronautics,
Langley Field, Vs., April 8, 1957.

[redacted]

REFERENCES

1. Chauvin, Leo T., and Speegle, Katherine C. : Boundary-Layer-Trans it ion and Heat -Transfer Measurements from Flight Tests of Blunt and Sharp 50° Cones at Mach Numbers From, 1.7 to 4.7. NACARM L57D04, 1957.

2. Garland, Benjamine J., and Chauvin, Leo T. : Measurements of Heat-Transfer and Boundary-Layer Transition on an 8-Inch-Diameter Hemisphere-Cylinder in Free Flight for a Mach Number Range of 2.00 to 3.88. NACA RM L57D04a, 1957.

3. Buglia, James J.: Heat Transfer and Boundary-Layer Transition on a Highly Polished Hemisphere-Cone in Free Flight at Mach Numbers Up to 3.14 and Reynolds Numbers Up to 24 x 10^6. NACA RM L57D05, 1957.

4. Rumsey, Charles B., and Lee, Dorothy B.: Measurements of Aerodynamic Heat Transfer and Boundary-Layer Transition on a 10° Cone in Free Flight at Supersonic Mach Numbers Up to 5.9. NACA RM L56B07, 1956.

5. Ginnings, Defoe C., and Thomas, Eugenia: The Electrical Resistance and Total Radiant Emittance of Inconel in the Range 0° to 1,000° C. NBS Rep. 4111 (NACA Contract S54-52), Nat. Bur. Standards, May 1955.

6. Wooley, Harold W.: Thermal Properties of Gases. Table 2.10, Nat. Bur. Standards, July 1949.

7. Chauvin, Leo T.: Pressure Distribution and Pressure Drag for a Hemispherical Nose at Mach Numbers 2.05, 2.54, and 3.04. NACA RM L52K06, 1952.

8. Ames Research Staff: Equations, Tables, and Charts for Compressible Flow. NACA Rep. 1135, 1953. (Supersedes NACA TN 1428.)

9. Stine, Howard A., and Wanlass, Kent: Theoretical end Experimental Investigation of Aerodynamic Heating and Isothermal Heat-Transfer Parameters on a Hemispherical Nose With Laminar Boundary Layer at Supersonic Mach Numbers. NACA TN 3344, 1954.

10. Van Driest, E. R.: Investigation of Laminar Boundary Layer in Compressible Fluids Using the Crocco Method. NACA TN 2597, 1952.

11. Van Driest, E. R.: Turbulent Boundary Layer in Compressible Fluids. Jour. Aero. Sci., vol. 18, no. 3, Mar. 1951, pp. 145-160, 216.

TABLE I.- LOCATION OF THERMOCOUPLES

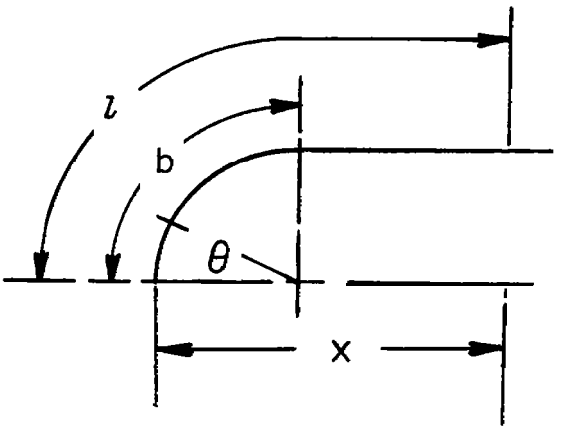

b=6.28 in.

Thermocouple number	0, deg	x, in.	l, in.	l/b	Skin thickness, in.
1	0	0	0	0	0.039
2	7.5	.04	.524	.083	.039
3	15	.15	1.05	.167	.039
4	30	.54	2.09	.333	.034
5	45	1.17	3.14	.500	.033
6	60	2.00	4.19	.667	.034
7	75	2.96	5.23	.834	.033
8	90	4.00	6.28	1.000	.027
9	-----	7.00	9.28	1.48	.033
[a]10	-45	1.17	3.14	.50	.033
[a]11	-60	2.00	4.19	.667	.034
[a]12	-90	4.00	6.28	1.00	.027
13		10.00	12.28	1.96	.034
14		14.00	16.28	2.59	.033
15		18.00	20.28	3.23	.034
16		22.00	24.28	3.86	.033
[a]17		7.00	9.28	1.48	.033
[a]18		10.00	12.28	1.96	.034
[a]19		14.00	16.28	2.59	.033
[a]20		18.00	20.28	3.23	.034

[a]180° from main line of thermocouples.

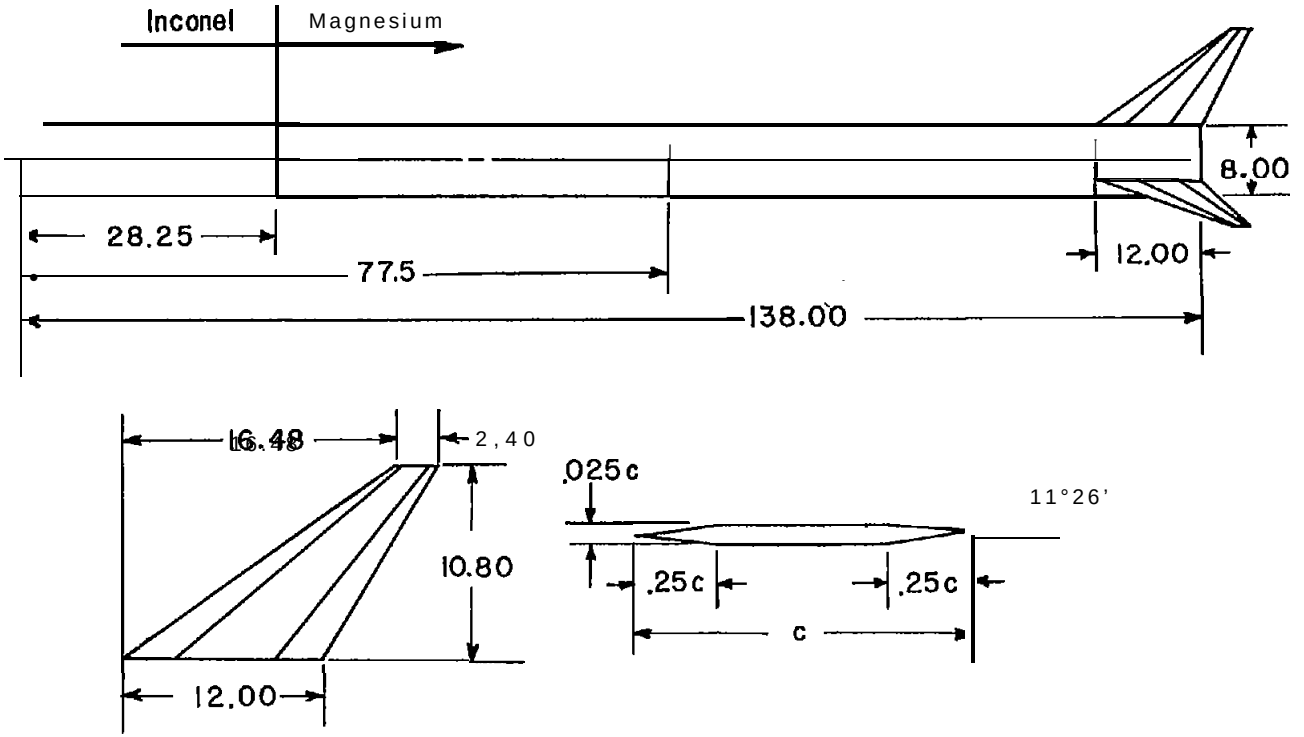

Figure 1.- Model configuration. All dimensions are in inches.

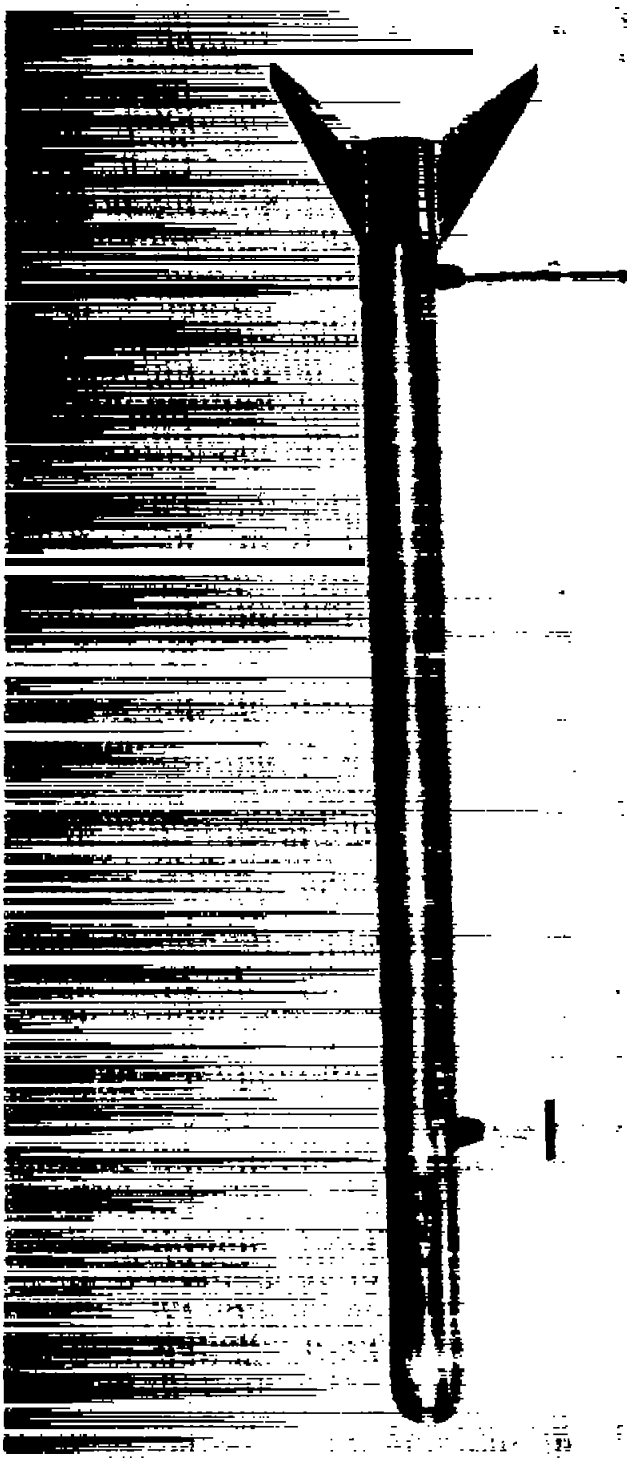

L-96984

Figure 2.- Photograph of model.

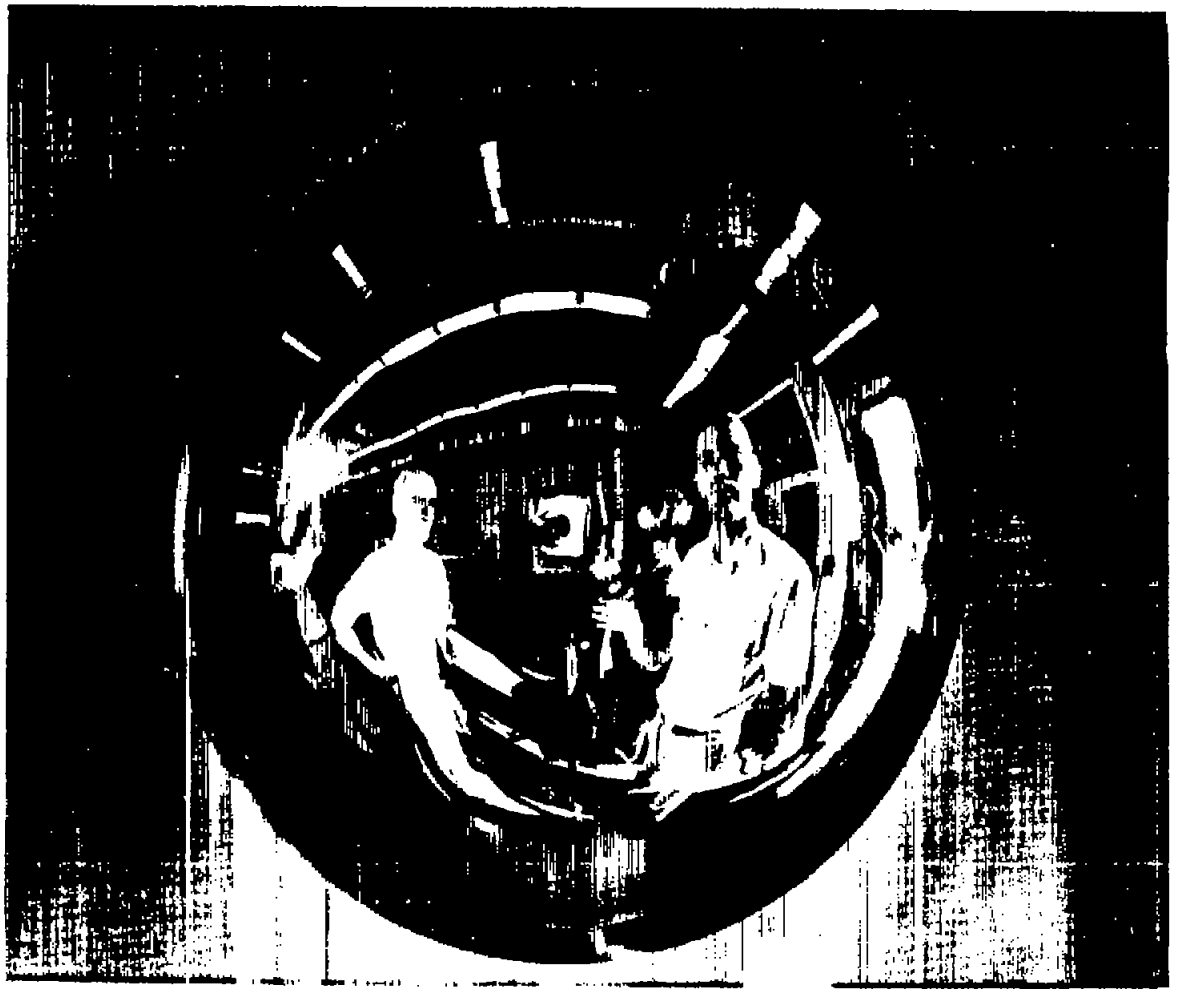

(a) Closeup of model nose. L-96983

Figure 3.- Photographs of model showing high degree of polish (0 to 5 microinches).

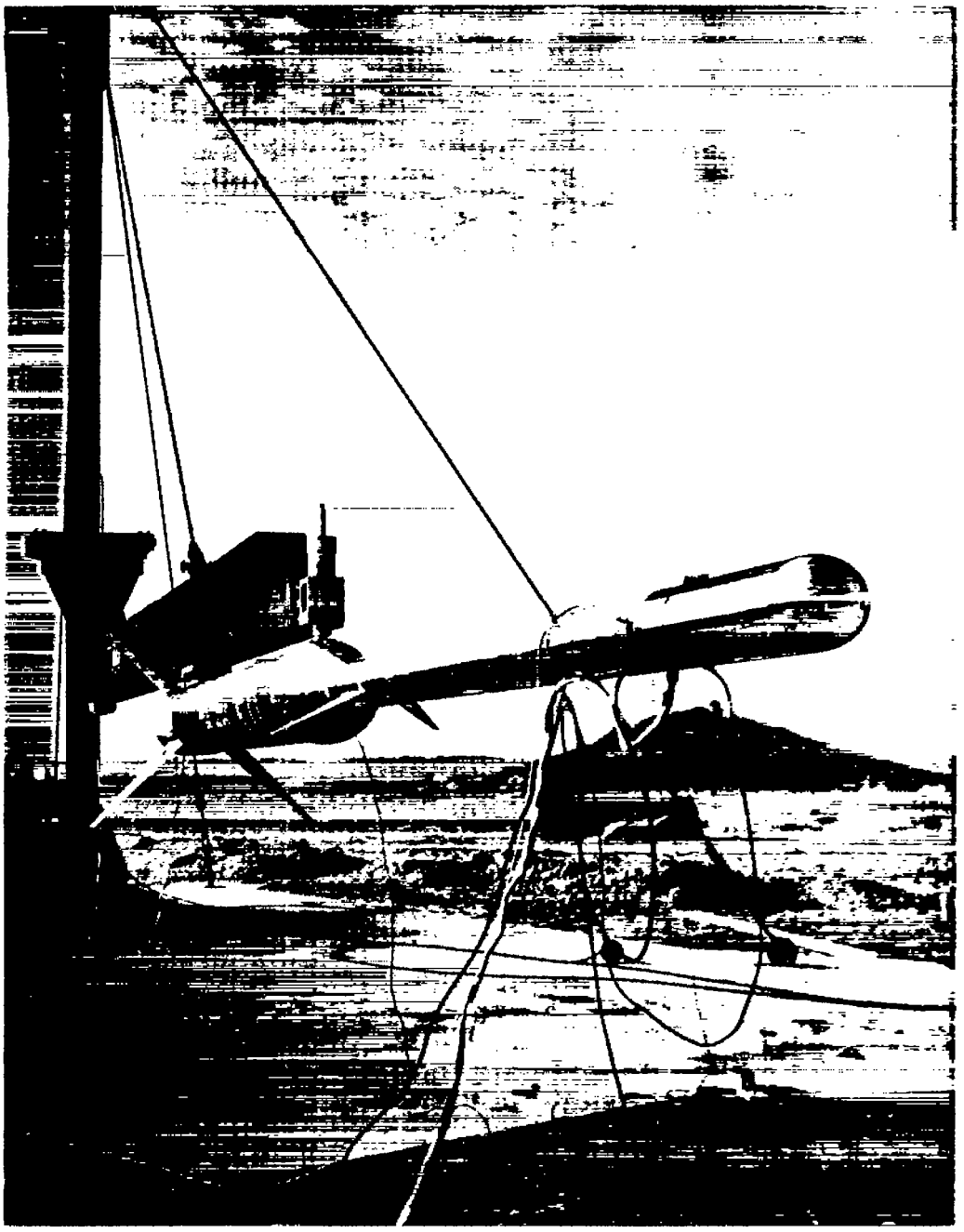

(b) Model mounted on launcher. L-97086

Figure 3.- Concluded.

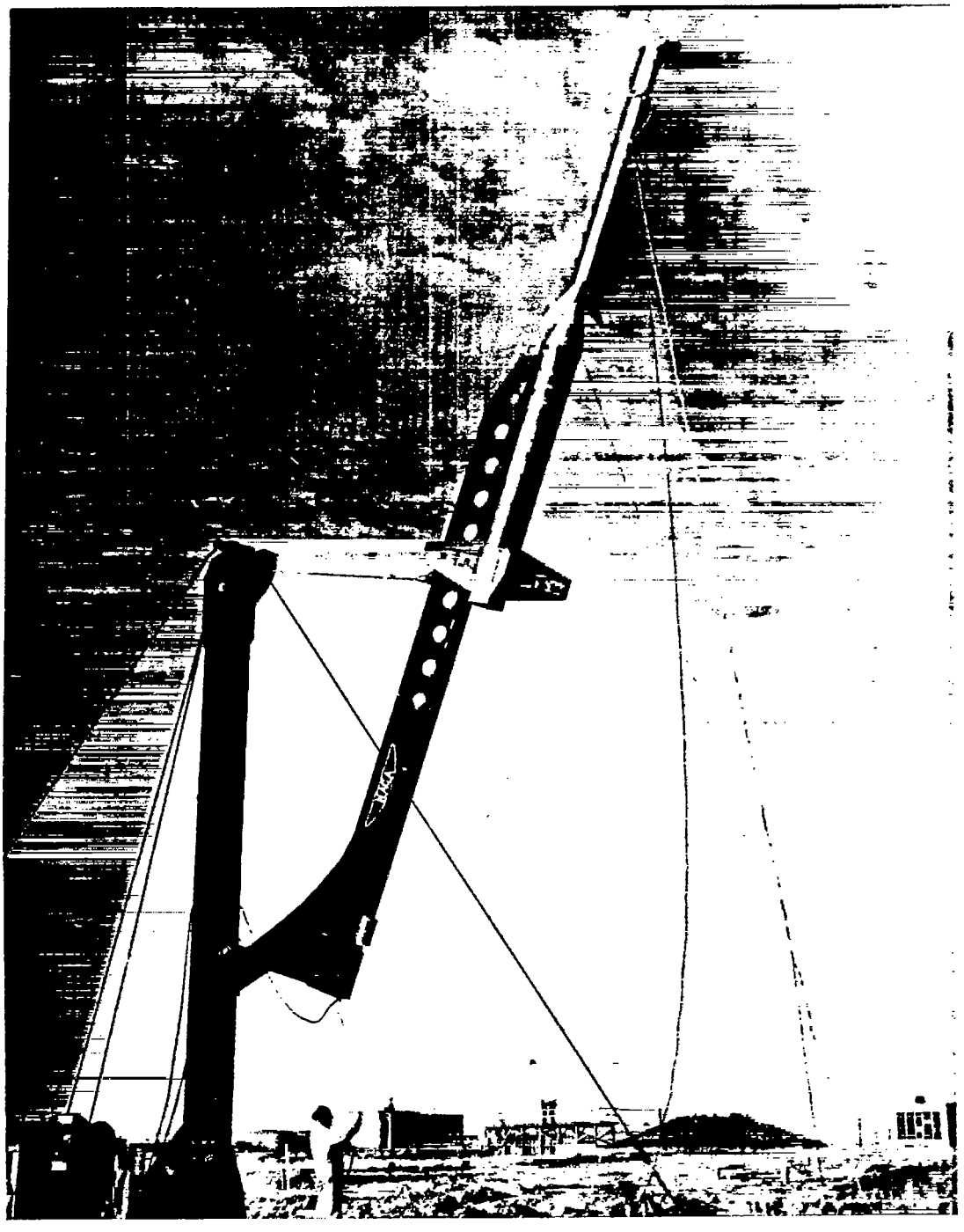

Figure 4.- Model-booster combination on launcher. L-97088

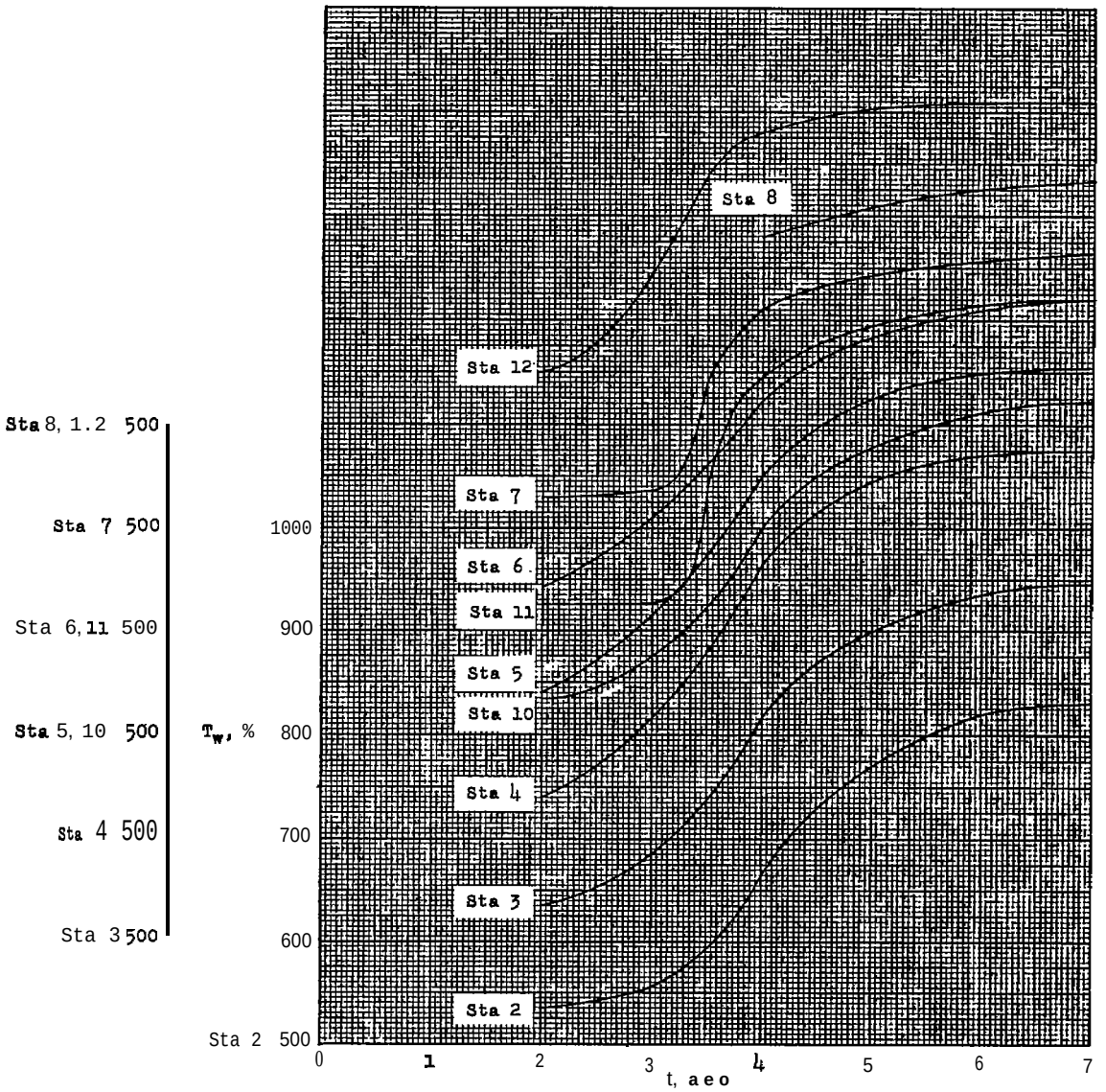

Figure 5.- Skin temperatures measured in flight.

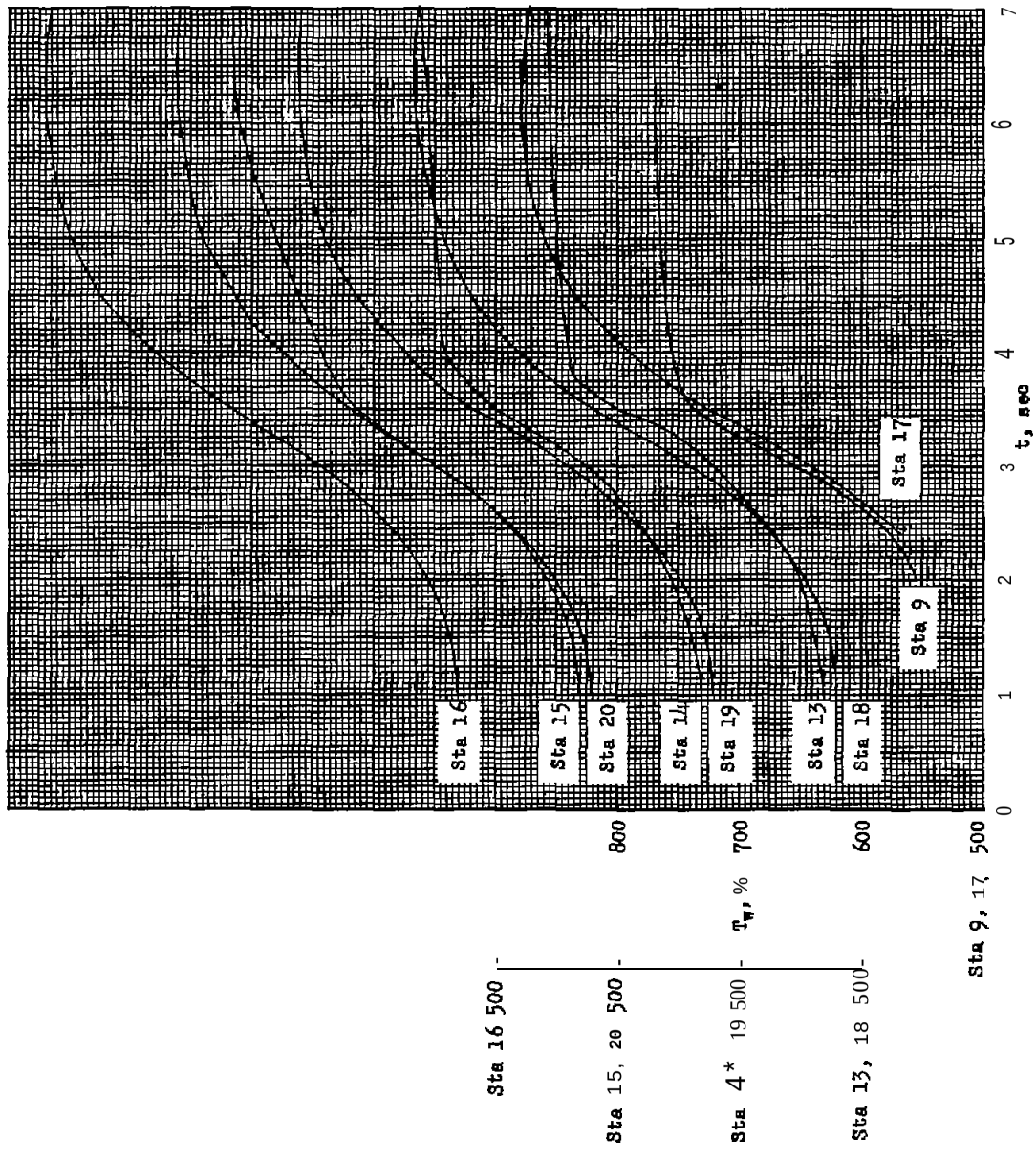

Figure 5.- Concluded.

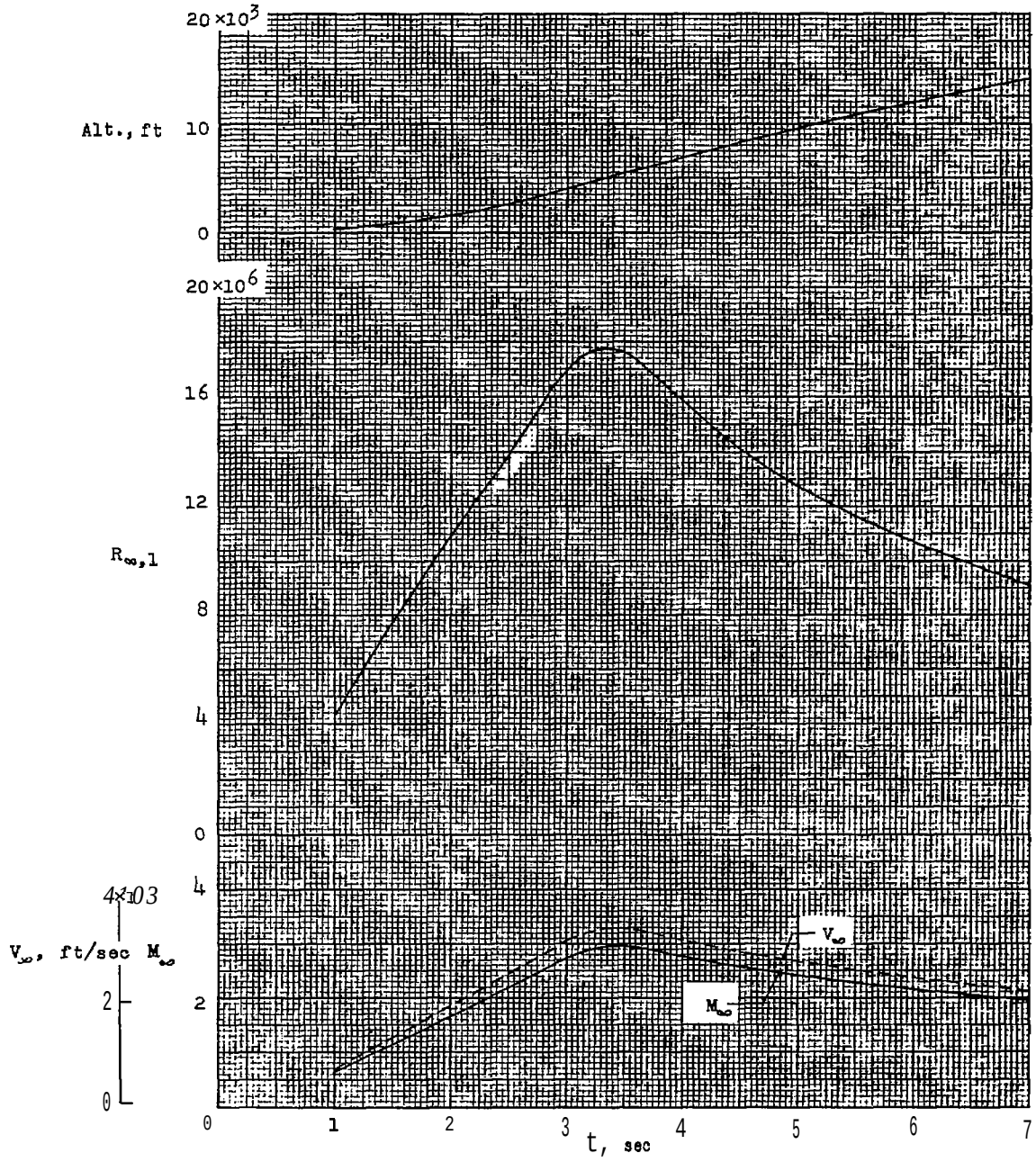

(a) Free-stream Mach number, velocity, Reynolds number based on length of 1 foot, and altitude.

Figure 6.- Test conditions.

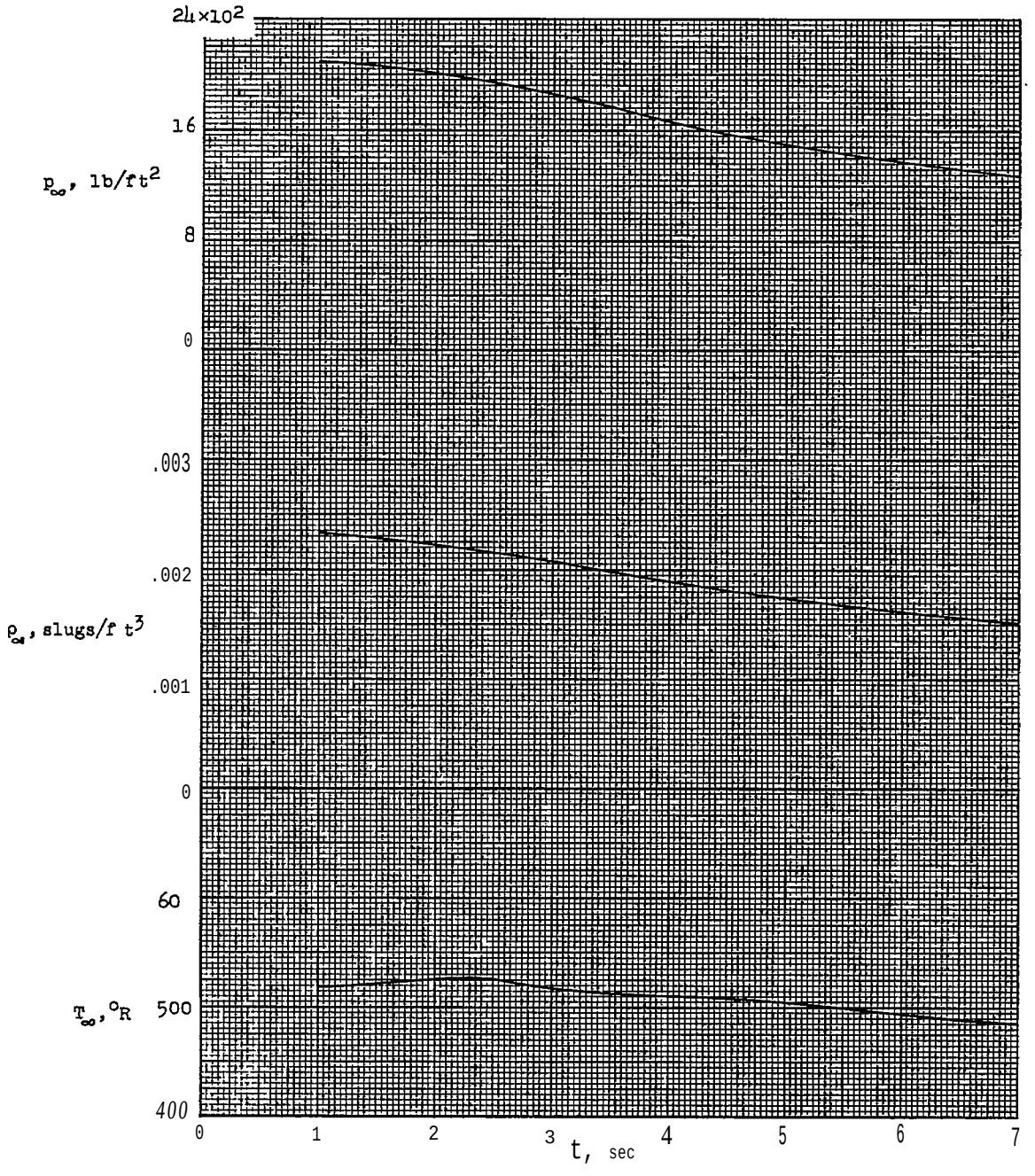

(b) Free-stream static temperature, density, and pressure.

Figure 6.- concluded.

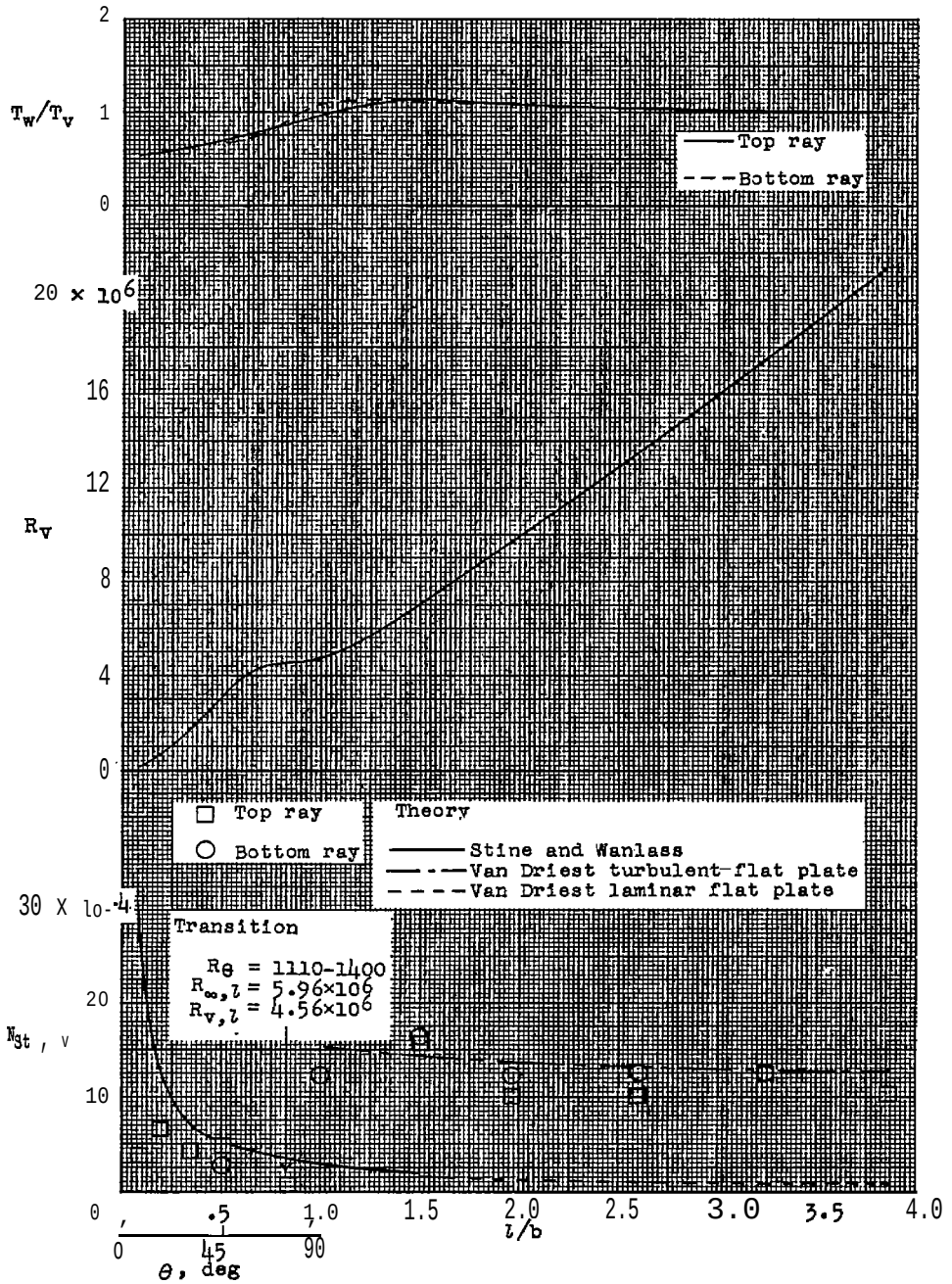

(a) t = 2.5; M = 2.14; $R_{\infty,l}$ = 13.7 x 10^6.

Figure 7.- Experimental and theoretical Stanton numbers, temperature ratios, and local Reynolds numbers based on distance from stagnation point.

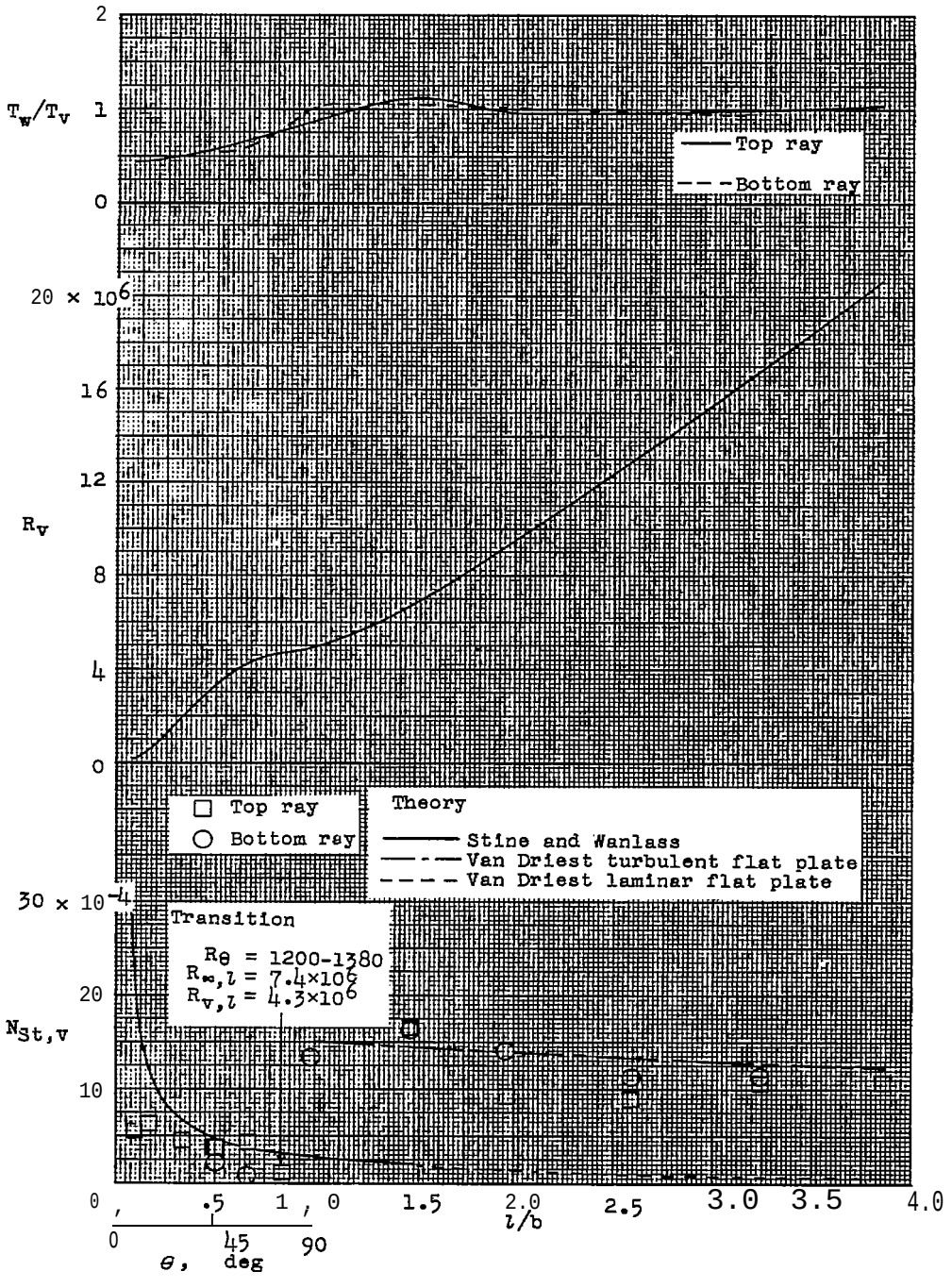

(b) t = 3.0; M = 2.73; $R_{\infty,l}$ = 17.0 x 10^6.

Figure 7.- Continued.

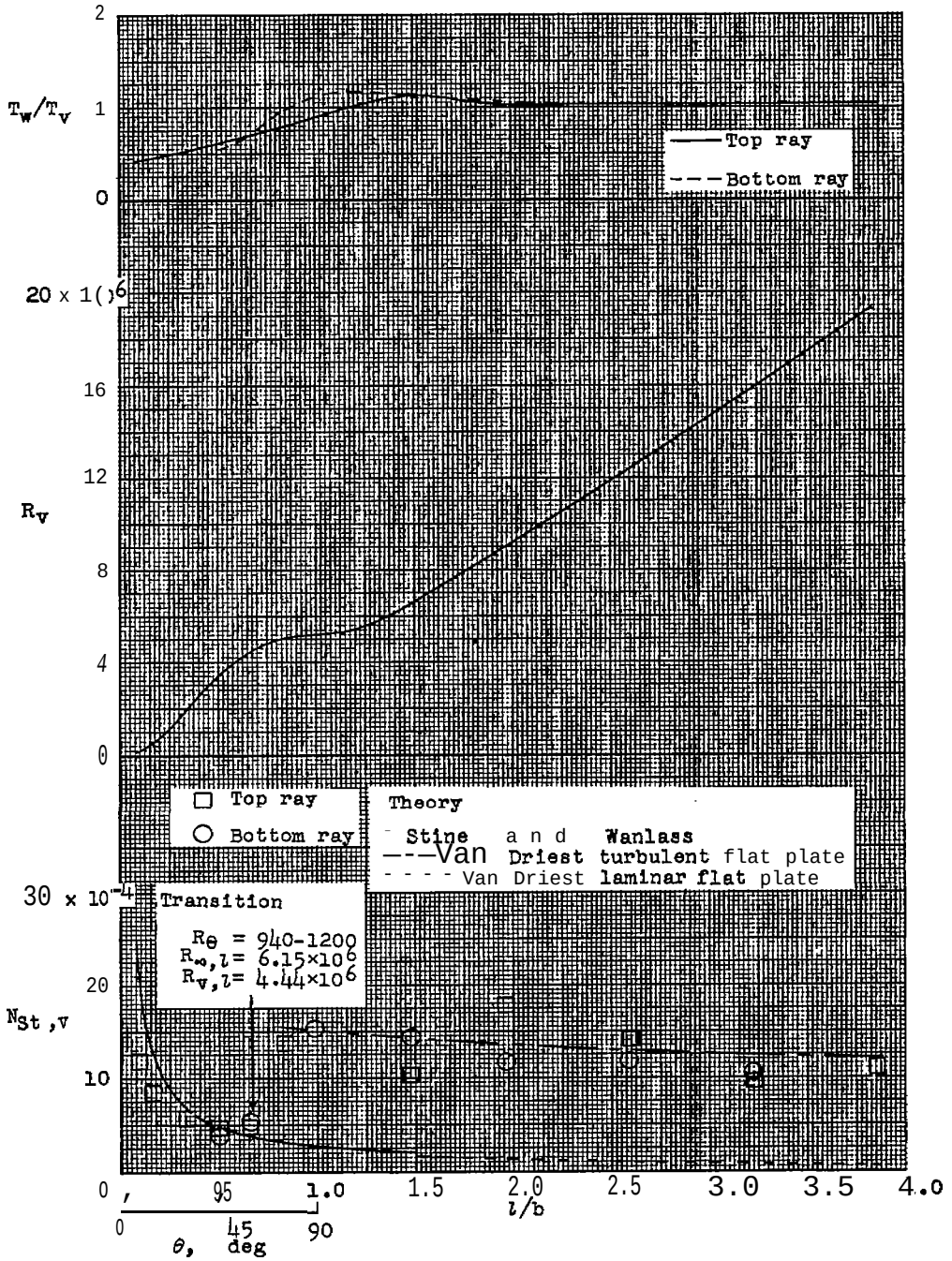

(C) t = 3.5; M = 2.96; $R_{\infty,1} = 17.7 \times 10^6$.

Figure 7.- Continued.

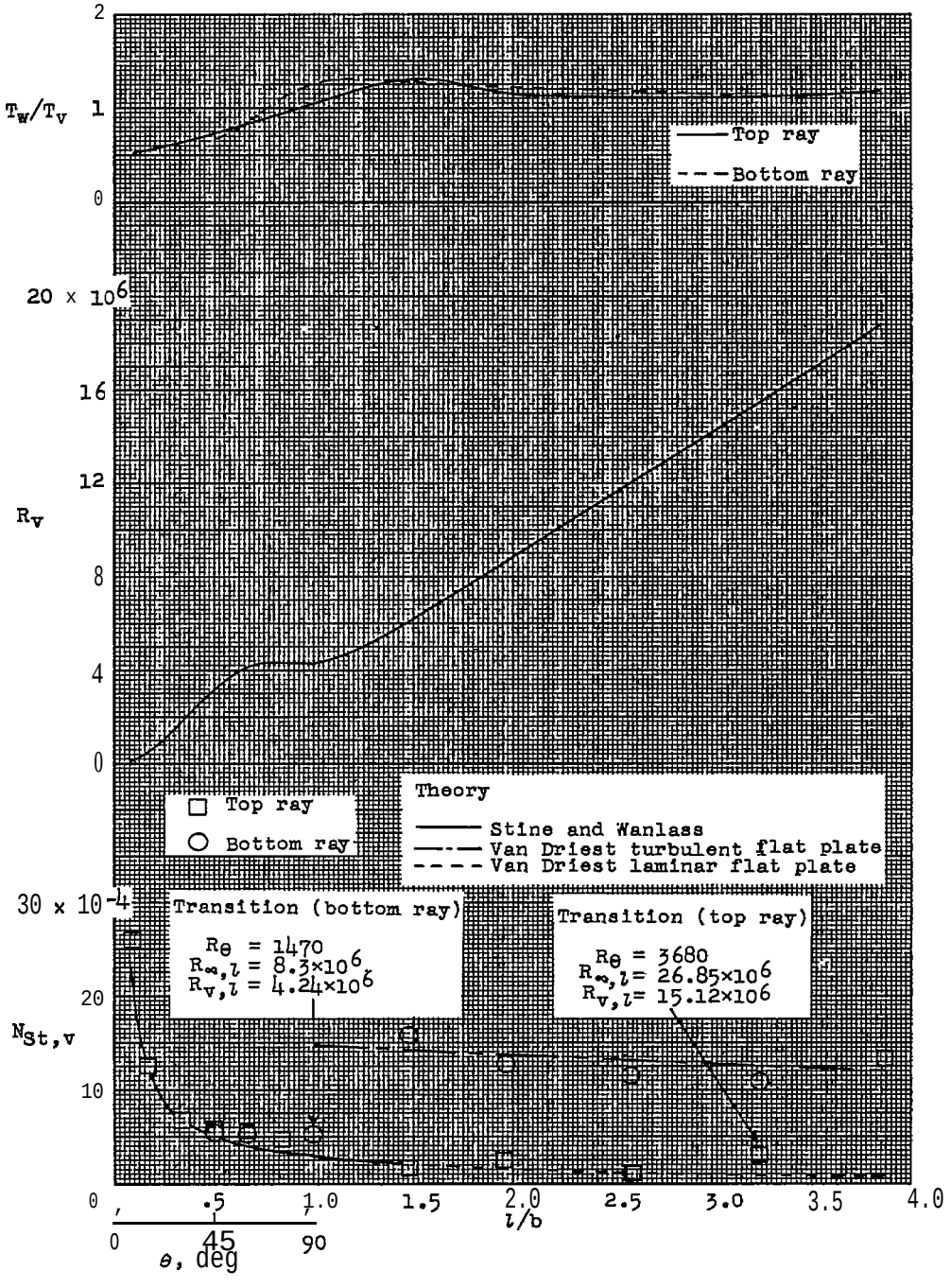

(d) t = 4.0; M = 2.78; $R_{\infty,l} = 15.9 \times 10^6$.

Figure 7.- Continued.

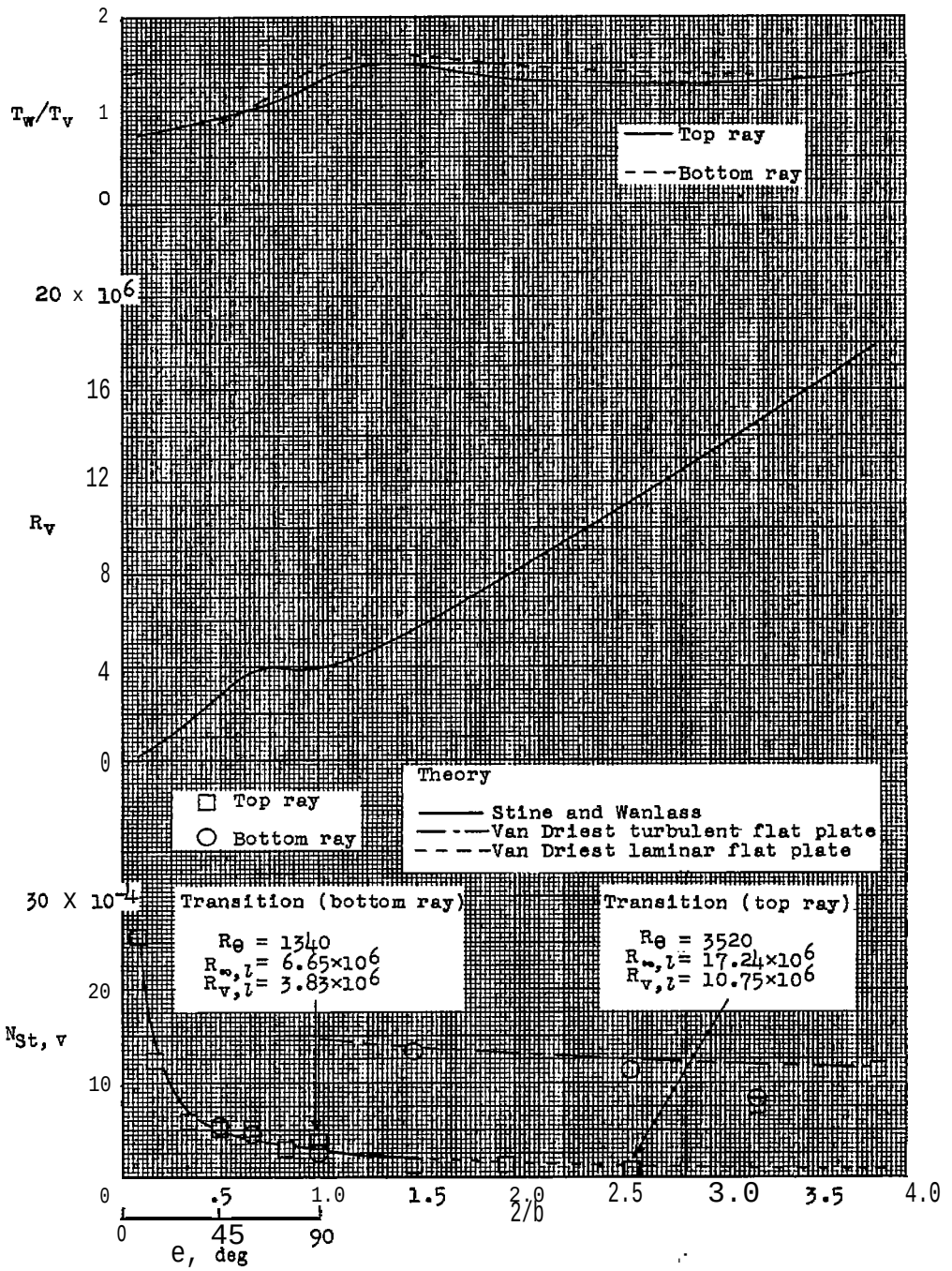

(e) t = 5.0; M = 2.42; $R_{\infty,1}$ = 12.7x 10^6.

Figure 7.- Continued.

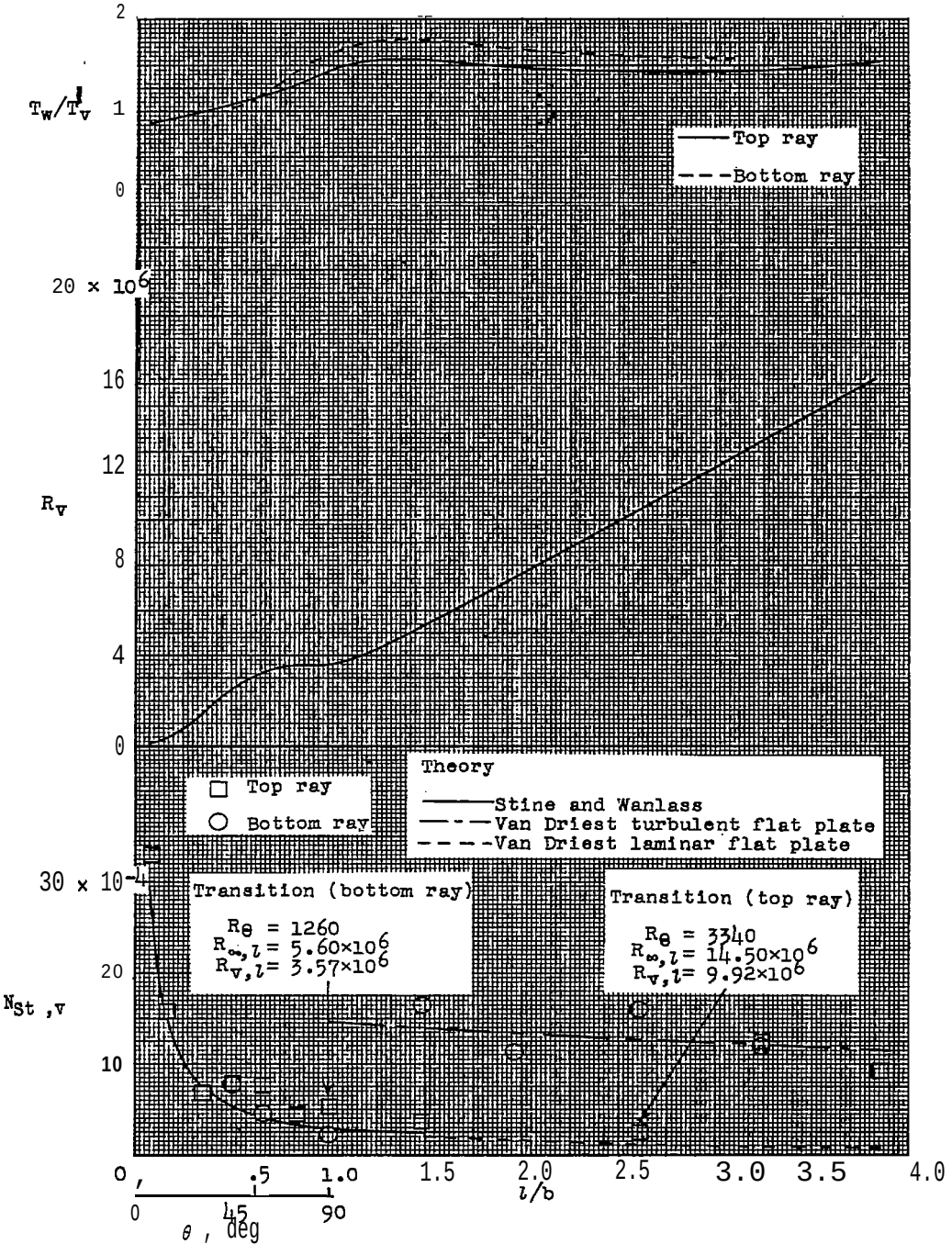

(f) t = 6.0; M = 2.17; $R_{\infty,l}$ = 10.7 x 10^6.

Figure 7.- Concluded.